Research Square

Preprints are preliminary reports that have not undergone peer review.
They should not be considered conclusive, used to inform clinical practice,
or referenced by the media as validated information.

Identification of a putative 2S albumin-like protein in an antifungal fraction from Capsicum chinense seeds

Arielle Pinheiro Bessiatti Fava Oliveira
Universidade Estadual do Norte Fluminense Darcy Ribeiro
Gabriela Martins Pereira
Universidade Estadual do Norte Fluminense Darcy Ribeiro
Larissa Maximiano Resende
Universidade Estadual do Norte Fluminense Darcy Ribeiro
Marcos Paulo Conceição Moura da Silva
Universidade Estadual do Norte Fluminense Darcy Ribeiro
Vitor Batista Pinto
Universidade Estadual do Norte Fluminense Darcy Ribeiro
Sarah Rodrigues Ferreira
Universidade Estadual do Norte Fluminense Darcy Ribeiro
Antonia Elenir Amancio Oliveira
Universidade Estadual do Norte Fluminense Darcy Ribeiro
Lorran Yves Machado Sousa
Universidade Estadual do Norte Fluminense Darcy Ribeiro
Ana Eliza Zeraik
Universidade Estadual do Norte Fluminense Darcy Ribeiro
Gabriel Bonan Taveira
Universidade Estadual do Norte Fluminense Darcy Ribeiro
Erica Oliveira Mello
Universidade Estadual do Norte Fluminense Darcy Ribeiro
André Oliveira Carvalho
Universidade Estadual do Norte Fluminense Darcy Ribeiro
Valdirene Moreira Gomes
valmg@uenf.br

Universidade Estadual do Norte Fluminense Darcy Ribeiro

Research Article

Keywords: Capsicum chinense, 2S albumin, seed storage proteins, antifungal activity, Candida, molecular docking.

Posted Date: November 24th, 2026

DOI: https://doi.org/10.21203/rs.3.rs-11613800/v1

License: This work is licensed under a Creative Commons Attribution 4.0 International License.
Read Full License

Additional Declarations: No competing interests reported.

Identification of a putative 2S albumin-like protein in an antifungal fraction from *Capsicum chinense* seeds

Arielle Pinheiro Bessiatti Fava Oliveira [1], Gabriela Martins Pereira[1], Larissa Maximiano Resende [1], Marcos Paulo da Conceição Moura da Silva [2], Vitor Batista Pinto [2], Sarah Rodrigues Ferreira [3], Antonia Elenir Amancio Oliveira [3], Lorran Yves Machado de Sousa [3], Ana Eliza Zeraik [3], Gabriel Bonan Taveira[1], Erica de Oliveira Mello[1], André de Oliveira Carvalho[1] and Valdirene Moreira Gomes [1]

[1] Laboratório de Fisiologia e Bioquímica de Microrganismos, Centro de Biociências e Biotecnologia, Universidade Estadual do Norte Fluminense Darcy Ribeiro, Campos dos Goytacazes, RJ, Brazil

[2] Laboratório de Biologia Celular e Tecidual, Centro de Biociências e Biotecnologia, Universidade Estadual do Norte Fluminense Darcy Ribeiro (UENF), Campos dos Goytacazes, RJ, Brazil

[3] Laboratório de Química e Função de Proteínas e Peptídeos, Centro de Biociências e Biotecnologia, Universidade Estadual do Norte Fluminense Darcy Ribeiro (UENF), Campos dos Goytacazes, RJ, Brazil

Correspondence: Valdirene Moreira Gomes *Address correspondence to this author at the Universidade Estadual do Norte Fluminense Darcy Ribeiro, Centro de Biociências e Biotecnologia, Campos dos Goytacazes, 28015-602, RJ, Brazil; Fax: +55-22-2726-1520; Email: valmg@uenf.br

Abstract

2S albumins are traditionally associated with nutrient storage but have also been linked to plant defense and antimicrobial activity. In this study, a protein fraction from *Capsicum chinense* seeds was investigated for the presence of a putative 2S albumin-like protein and its antifungal potential. Seed proteins were fractionated by ion-exchange and reversed-phase chromatography, and fraction P1' was selected for further characterization based on its chromatographic profile. LC-MS/MS analysis identified three peptide fragments with 100% sequence identity to corresponding regions of a 2S albumin-like protein from *C. annuum*, supporting their assignment to this protein family. Structural modeling and phylogenetic analysis provided additional support for this assignment. The antifungal activity of fraction P1' was evaluated against *Candida albicans* and *Candida tropicalis*, yielding IC_{50} values ranging from 3.12 to 6.25 μg mL^{-1} and from 6.25 to 12.5 μg mL^{-1}, respectively. Additional assays indicated species-dependent cellular responses, including intracellular reactive oxygen species production and mitochondrial membrane depolarization in *C. tropicalis*. Dynamic light scattering suggested changes in particle-size distribution in the presence of a model lipid system, while molecular docking predicted favorable interactions between the modeled 2S albumin-like structure and representative fungal cell-envelope components. Although these findings support the presence of a putative 2S albumin-family protein in fraction P1', the purity of the preparation could not be independently confirmed by electrophoresis. The results therefore establish the antifungal potential of the fraction and provide a basis for further investigation of the identified protein candidate and its possible biological role.

Keywords

Capsicum chinense; 2S albumin; seed storage proteins; antifungal activity; *Candida*; molecular docking.

1. Introduction

The colonization of terrestrial environments by plants was marked by major evolutionary innovations, among which the formation of seeds stands out as one of the most significant events [1]. In addition to protecting the embryo, seeds are highly specialized structures responsible for the synthesis and storage of proteins within reserve tissues and protective seed coats, thereby supporting reproduction, dispersal, and species establishment in diverse environments [2]. During seed maturation, extensive accumulation of storage compounds occurs, particularly carbohydrates, lipids, and proteins, a process that is essential for the acquisition of desiccation tolerance, the establishment of dormancy, and the provision of energy and nutrients required for germination and early seedling development. The high protein content can subsequently be mobilized and utilized for plant maintenance, defense, and growth [3].

Among the compounds accumulated during maturation, seed storage proteins (SSPs) play a central role in both plant physiology and human and animal nutrition [4]. These proteins represent major sources of nitrogen, carbon, and sulfur and are synthesized during the seed-filling and maturation stages and subsequently mobilized during germination to meet the metabolic demands of the embryo until autotrophic growth is established [5]. Based on their solubility properties, SSPs have traditionally been classified into albumins, globulins, prolamins, and glutelins [4,6].

However, this solubility-based classification does not adequately reflect the structural and functional relationships among these proteins. Therefore, more recent classification approaches have considered the conservation of amino acid sequences, three-dimensional structures, and biological activities, allowing SSPs to be grouped into three major families: prolamins, cupins, and Bet v 1-related or pathogenesis-related proteins [7].

The prolamin family is characterized by conserved cysteine residues and a predominance of α-helical structures and includes proteins such as 2S albumins, nonspecific lipid transfer proteins (nsLTPs), cereal prolamins, and α-amylase inhibitors. Within this context, some storage proteins, including 2S albumins,

nsLTPs, and members of the cupin family, are also associated with food allergies, highlighting their functional diversity beyond their conventional role as nutrient sources during germination [8].

Among these proteins, 2S albumins are distinguished by the structural stability conferred by disulfide bonds and their widespread occurrence in seeds, particularly those of dicotyledonous plants. They are low-molecular-weight proteins generally synthesized as precursors of approximately 18–24 kDa that undergo proteolytic processing during seed maturation, generating a small subunit of approximately 3–4 kDa and a large subunit of 8–10 kDa. These subunits are stabilized by four disulfide bonds formed between eight conserved cysteine residues. In addition, 2S albumins are characterized by high contents of glutamine, arginine, asparagine, and cysteine and generally exhibit a cationic nature, properties that contribute to their physicochemical characteristics and structural stability [5].

Although initially described as storage proteins, accumulating evidence over recent decades has demonstrated that these proteins perform a much broader range of biological functions. In addition to serving as nutrient reserves during germination, several 2S albumins participate in the regulation of reserve mobilization through the inhibition of hydrolytic enzymes, such as α-amylases and serine proteases, thereby preventing the premature degradation of storage compounds and contributing to the physiological control of germination [9]. Furthermore, 2S albumins exhibit antifungal, antibacterial, insecticidal, and antiviral activities, highlighting their important role in seed defense mechanisms against phytopathogenic microorganisms and insect predators [5].

The increasing incidence of human diseases caused by fungi, together with the growing resistance to conventional antifungal agents and the demand for naturally derived molecules, has driven the search for plant proteins with antimicrobial properties [10]. In this context, defense proteins present in seeds have attracted considerable interest because of their high stability, structural diversity, and biotechnological potential. These proteins may represent promising alternatives for the development of novel antifungal agents with applications in agriculture and, potentially, in the biomedical field.

Species belonging to the genus *Capsicum* are of recognized economic and nutritional importance and are widely cultivated in different regions of the world. However, *Capsicum* seeds remain relatively underexplored, despite representing a rich source of proteins and other potentially bioactive biomolecules [11]. Although an increasing number of studies have investigated the chemical composition and biological properties of *Capsicum* fruits, knowledge of the proteins present in their seeds remains limited, particularly with regard to 2S albumins. To date, there have been no reports on the purification, structural identification, and functional characterization of 2S albumins from *Capsicum chinense* seeds, highlighting an important gap in our understanding of the bioactive proteins of this species.

Against this background, the present study aimed to investigate the presence of a putative 2S albumin-like protein in a fraction obtained from *C. chinense* seeds and to evaluate the antifungal activity of this fraction against *Candida albicans* and *Candida tropicalis*. The fraction was characterized by LC-MS/MS, sequence comparison, and structural modeling to assess the association of the identified peptide fragments with the 2S albumin family. This approach provides evidence for the occurrence of a putative 2S albumin-like protein in *C. chinense* seeds and explores the antifungal potential of the corresponding chromatographic fraction.

2. Materials and methods

2.1 Seeds of *C. chinense*

Seeds of *C. chinense* Jacq. (accession UENF 1751) used in this study were provided by the Plant Breeding Laboratory of the Center for Agricultural Sciences and Technologies at the Universidade Estadual do Norte Fluminense Darcy Ribeiro (UENF), Campos dos Goytacazes, Rio de Janeiro, Brazil. Pepper plants were cultivated as previously described [12]. Ripe fruits were harvested 45 days after anthesis, and the seeds were carefully removed, manually separated, air-dried at room temperature, and used for protein extraction experiments.

2.2 Microorganisms

The yeasts *Candida albicans* (CE022) and *Candida tropicalis* (CE017), used in the antifungal assays, were obtained from the Department of Biology of the Universidade Federal do Ceará (UFC), Fortaleza, Ceará, Brazil. The strains were

maintained on Sabouraud agar medium (1% peptone, 2% glucose, and 1.7% agar; Merck) at the Laboratory of Physiology and Biochemistry of Microorganisms, UENF.

2.3 Seed Protein Extraction

Seed proteins from *C. chinense* were obtained according to the methodology described by [12]. The seeds were ground in liquid nitrogen until a fine powder was obtained. Subsequently, 5 g of the powder were added to a buffer consisting of 0.01 M Na_2HPO_4, 0.015 M NaH_2PO_4, 0.1 M KCl, and 1.5% EDTA, adjusted to pH 5.4, at a 1:10 (w/v) ratio. The suspension was continuously stirred for 2 h at 4 °C. The material was then centrifuged at 7,830 × *g* for 45 min at 4 °C. The resulting supernatant was collected, filtered, and subjected to protein precipitation with ammonium sulfate at 70% saturation. The mixture was allowed to stand for 16 h at 4 °C to allow protein precipitation. The protein precipitate was recovered by centrifugation and subsequently subjected to heat treatment at 80 °C for 15 min. A second centrifugation was then performed to remove the precipitated thermolabile proteins and other components. The resulting supernatant was collected and dialyzed against distilled water for 72 h. Finally, the dialyzed material was lyophilized, yielding the seed protein extract (SPE).

2.4 Chromatographic Fractionation of the Seed Protein Extract

The separation of proteins present in the SPE was performed by ion-exchange chromatography followed by reversed-phase high-performance liquid chromatography (RP-HPLC), as described by [12]. Initially, 50 mg of SPE were solubilized in 100 mM Tris-HCl buffer, pH 8.0, and subjected to anion-exchange chromatography on a DEAE-Sepharose resin. The unretained fraction, designated C1, was collected and subsequently subjected to RP-HPLC.

For RP-HPLC separation, an HIBAR LiChrosorb® RP-18 C18 column (25 × 0.46 cm; 5 µm; Merck), preceded by a Pelliguard LC-18 C18 guard column (Supelco), was used. The C1 fraction was solubilized in ultrapure water at a concentration of 1 mg/mL. Chromatographic separation was performed using solvent A, consisting of water containing 8.77 mM trifluoroacetic acid (TFA), and solvent B, consisting of propanol containing 8.77 mM TFA. Analyses were

conducted at 40 °C with a flow rate of 0.5 mL min^{-1}. Initially, the column was maintained at 100% solvent A for 15 min, followed by a linear gradient from 0 to 50% solvent B from 15 to 115 min. At the end of the elution, the column was re-equilibrated with 100% solvent A. Eluted components were monitored at 280 nm using a diode-array detector (DAD). The initial separation by RP-HPLC yielded ten chromatographic peaks, designated P1–P10, as previously described [12].

Fraction P1 was then subjected to a second separation step via RP-HPLC to obtain fraction P1' for subsequent analyses. In this stage, the column was initially held at 100% solvent A for approximately 7 min, followed by a linear gradient of solvent B (from 0% to 50%), as shown in the chromatographic profile in Figure 1. The eluted components were monitored at 220 nm, as recorded in the chromatogram. The fraction corresponding to peak P1' was collected for further molecular characterization and evaluation of its antifungal activity.

2.6 Mass Spectrometry and Data Analysis

The identification and characterization of the protein fragments were performed by liquid chromatography-tandem mass spectrometry (LC-MS/MS). For this purpose, the protein fragments were subjected to disulfide bond reduction, cysteine residue alkylation, and enzymatic digestion with trypsin, as described below.

For disulfide bond reduction, the fragments were incubated with 10 mM dithiothreitol (DTT) prepared in 100 mM ammonium bicarbonate (AmBic) for 30 min at 55 °C under agitation. After removal of the reducing solution and a subsequent dehydration step, cysteine alkylation was performed using 55 mM iodoacetamide (IAA; Merck) prepared in 100 mM AmBic. The samples were protected from light and incubated for 30 min at room temperature. Subsequently, the fragments were incubated with trypsin solution (Promega, V5111) at an enzyme-to-protein ratio of 1:100, prepared in 10 mM AmBic containing 10% ACN. Digestion was initially performed at 4 °C for 30 min, followed by incubation at 37 °C for 18 h.

The generated peptides were recovered using a 5% formic acid solution in ACN (1:2, v/v) and incubated at 37 °C for 30 min. Following extraction, the samples

were concentrated using a vacuum concentrator (SpeedVac) and resuspended in 0.1% formic acid prepared in 50 mM AmBic before chromatographic and mass spectrometric analyses.

LC-MS/MS analyses were performed using a nanoAcquity UPLC system (Waters, Manchester, UK) coupled to a Synapt G2-Si HDMS mass spectrometer (Waters). Approximately 2 µg of peptides were injected per analysis. Initially, the samples were concentrated on a C18 trapping column (180 µm × 20 mm; 5 µm, Waters) for 3 min at a flow rate of 5 µL min^{-1}. Chromatographic separation was performed on a nanoAcquity HSS T3 C18 column (75 µm × 150 mm; 1.8 µm) maintained at 45 °C and operated at a flow rate of 400 nL min^{-1}. The mobile phases consisted of water containing 0.1% formic acid (mobile phase A) and acetonitrile containing 0.1% formic acid (mobile phase B). Elution was performed using a linear gradient from 7 to 40% mobile phase B over 92.72 min, followed by an increase to 99.9% at 106 min and column re-equilibration to the initial conditions until completion of the 120-min analysis.

Mass spectra were acquired in positive ion mode using data-independent acquisition (DIA) combined with ion mobility separation. The main instrumental parameters included an ion mobility wave velocity of 600 m s^{-1}, a collision energy ramp of 19–55 V for high-energy acquisition, a source temperature of 70 °C, a cone voltage of 30 V, and a capillary voltage of 2.75 kV. TOF scans were acquired over an *m/z* range of 50–2000, with an acquisition time of 0.5 s. Human [Glu^1]-fibrinopeptide B (Sigma-Aldrich; 100 fmol μL^{-1}) was used as a reference standard for lock-mass correction, with automatic calibration performed every 30 s.

2.7 Phylogenetic Analysis of 2S Seed Storage Proteins

Homologous protein sequences belonging to the 2S seed storage protein family were retrieved from the NCBI Protein database, using the predicted *Capsicum annuum* protein (XP_047265719.1) as the reference sequence. To avoid potential biases arising from the presence of fused sequences or proteins of different lengths, a second analysis was performed using only orthologous proteins corresponding to the homologous region experimentally identified in this study.

The selected sequences were obtained from *C. annuum*, *Capsicum galapagoense*, *Nicotiana tabacum*, *Nicotiana tomentosiformis*, *Lycium barbarum*, and *Solanum stenotomum*. Multiple sequence alignment was performed using the ClustalW algorithm implemented in MEGA version 12.

The best-fit evolutionary model was selected using the Find Best Protein Models (ML) tool available in MEGA12, with the Bayesian Information Criterion (BIC) used as the model selection criterion. For the orthologous protein dataset, the cpREV+G+F model exhibited the lowest BIC value and was therefore selected for phylogenetic reconstruction.

The phylogenetic tree was inferred using the Maximum Likelihood method under the cpREV+G+F model, with a gamma distribution with five discrete categories to account for among-site rate heterogeneity and empirical amino acid frequencies (+F). The reliability of the inferred clusters was assessed using 1,000 bootstrap pseudoreplicates.

2.8 Dynamic Light Scattering (DLS)

The hydrodynamic diameter of the P1' fraction was determined by dynamic light scattering (DLS) using a Dynamic Light Scattering instrument (Kaliope). Analyses were performed with the protein at a concentration of 500 µM, in the absence and presence of the POPS/POPC/POPE/Erg membrane model (28/21/21/30 mol%), prepared in Tris-HCl buffer at pH 7.5.

The samples were transferred to appropriate DLS cuvettes and analyzed at a controlled temperature of 25 °C. For each experimental condition, 60 independent measurements were performed.

Data were acquired and processed using the instrument software to determine the mean hydrodynamic diameter (Z-average) and polydispersity index (PDI). As experimental controls, samples containing only the buffer and only the membrane model were analyzed under the same experimental conditions.

2.9 Antifungal Activity of the *Cc*-Alb2S

The antifungal activity of the P1' fraction was evaluated against *C. albicans* and *C. tropicalis* using an adaptation of the methodology described by [13]. The yeasts were initially cultured on Sabouraud agar (Merck) for 24 h at 30 °C. The cells were then resuspended in Sabouraud broth and quantified using a Neubauer counting chamber.

Cell suspensions containing 1 × 10^4 cells mL^{-1} were incubated in 96-well plates containing 100 µL of Sabouraud broth and different concentrations of the *Cc*-Alb2S (0.78–100 µg mL^{-1}), in a final reaction volume of 200 µL. For both species, antifungal activity was initially evaluated at a concentration of 100 µg mL^{-1} after 24 h of incubation at 30 °C. Based on the results obtained, the half-maximal inhibitory concentrations (IC_{50}) were determined by nonlinear regression.

Cell growth was determined by measuring absorbance at 620 nm using a microplate reader (EZ Read 400, Biochrom). The percentage of growth inhibition was calculated by considering the control group as representing 100% growth, according to the following equation:

$$\text{Inhibition (\%)} = 100 - (tABS_{620} \times 100 / cABS_{620})$$

where $tABS_{620}$ corresponds to the mean absorbance measured at 620 nm of samples treated with the *Cc*-Alb2S after 24 h of incubation, whereas $cABS_{620}$ corresponds to the mean absorbance measured at 620 nm of samples from the control group after the same incubation period.

2.10 Membrane Permeabilization Assay (SYTOX Green)

Plasma membrane permeabilization was assessed using the fluorescent probe SYTOX Green. The assay was performed based on the methodology described for the fungal growth inhibition assay, with specific adaptations for the analysis of membrane integrity.

After 15 h of incubation with the *Cc*-Alb2S, *C. albicans* and *C. tropicalis* cells were treated with the IC_{50} concentrations determined based on the values obtained in the growth inhibition assay.

Subsequently, the samples were incubated with 0.2 µM SYTOX Green for 15 min at 30 °C in the dark [14,15]. Untreated cells were used as the negative control, whereas cells subjected to heat treatment at 100 °C for 1 min prior to probe addition were used as the positive control.

The samples were analyzed by fluorescence and differential interference contrast (DIC) microscopy using an Axioplan A2 microscope (Zeiss) equipped with a fluorescein filter (excitation: 450–490 nm; emission: 500 nm). Acquisition parameters were standardized using the positive control and kept constant for all samples.

2.11 Determination of Intracellular Reactive Oxygen Species (ROS)

Intracellular production of reactive oxygen species (ROS) was determined using the fluorescent probe 2′,7′-dichlorofluorescein diacetate (H_2DCFDA) [15]. After 15 h of incubation with the P1' fraction at the IC_{50} concentrations determined for *C. albicans* and *C. tropicalis*, respectively, the samples were incubated with 20 µM H_2DCFDA for 30 min at 30 °C, protected from light and under constant agitation. Cells treated with 3% acetic acid were used as the positive control, whereas untreated cells were used as the negative control [15].

Fluorescence was analyzed using an Axioplan A2 microscope (Zeiss) equipped with a fluorescein filter (excitation: 450–490 nm; emission: 500 nm). DIC images were also acquired to assess cellular morphology. Acquisition parameters were kept constant throughout all analyses.

2.12 Evaluation of Mitochondrial Membrane Potential (JC-1)

Mitochondrial membrane potential was evaluated using the fluorescent probe JC-1 [16]. After 15 h of incubation with the P1' fraction at the IC_{50} concentrations determined for *C. albicans* and *C. tropicalis*, respectively, the samples were incubated with 5 µM JC-1 for 40 min at 37 °C, protected from light. Cells incubated with the probe alone were used as the negative control [16].

Analyses were performed by fluorescence and differential interference contrast (DIC) microscopy using an Axioplan A2 microscope (Zeiss) equipped with

appropriate filters for the detection of JC-1 monomers (green fluorescence) and aggregates (red fluorescence). Acquisition parameters were kept constant for all samples.

2.13 Structural Modeling of the P1' 2S Albumin-Like Protein

The three peptide fragments experimentally identified in *Cc*-Alb2S were subjected to BLASTp searches and subsequently aligned using Clustal Omega (https://www.ebi.ac.uk/jdispatcher/msa/clustalo). The hypothetical protein P3S67_003004 from *Capsicum chacoense* (KAM3321853.1) was selected for homology modeling using SWISS-MODEL (https://swissmodel.expasy.org/), with the 2S seed storage albumin-like protein from *Nicotiana tabacum* (A0A1S4BWM1.1.A; 81.94% sequence identity) as the template.

The resulting model was structurally aligned with the experimentally determined Ara h 6 2S albumin (PDB ID: 8SJA, chain D) to assess conservation of the characteristic 2S albumin fold and delimit the corresponding structural domain for subsequent molecular docking analyses.

2.14 Molecular Docking with Representative Fungal Cell Wall and Membrane Components

Molecular docking analyses were performed to investigate potential interactions between the modeled 2S albumin-like protein and representative components of the *Candida* cell envelope. The selected ligands included chitotetraose ($GlcNAc_4$; PDB ID: 1LZR), α-1,2-mannobiose (Man_2; PDB ID: 1I3H), laminaritriose and 6-O-glucosyl-laminaritriose (PDB ID: 2W52), and ergosterol (PubChem CID: 444679).

Docking was performed using the DockThor server (https://dockthor.lncc.br/v2/) with a blind-docking approach and a 40 × 40 × 40 Å search grid. Docking solutions were clustered according to their spatial distribution, and the lowest-energy pose within the most populated binding region was selected for further analysis. Protein–ligand interactions were characterized using PLIP [17].

3. Results

3.1 Chromatographic Fractionation of Seed Proteins from *C. chinense*

The seed protein extract (SPE) from *C. chinense* was subjected to anion-exchange chromatography followed by reversed-phase high-performance liquid chromatography (RP-HPLC) to separate and enrich its protein components [12]. The selected P1 fraction was subsequently re-chromatographed, yielding a single major chromatographic peak designated P1'. This peak eluted at 6 min under the chromatographic conditions employed, indicating low retention on the C18 stationary phase. The presence of a single major peak suggests an apparently homogeneous chromatographic profile under the conditions used; however, this observation alone does not establish the presence of a single protein. Fraction P1' was therefore selected for subsequent molecular characterization and antifungal evaluation, and its chromatographic profile is shown in Fig. 1. Thus, the results presented below focus on the characterization and evaluation of fraction P1', aiming to further elucidate its biochemical properties and biological potential.

3.2 Characterization of Fraction P1' by Mass Spectrometry

Trypsin digestion of fraction P1' followed by mass spectrometric analysis identified three peptide fragments corresponding to the sequences CCQQLQQVQDPQCR, QVFQQEQQR, and QQMLQTAQNLPGLCK. These peptide fragments were aligned and compared against protein databases, revealing similarity to 2S albumin-type proteins from *C. annuum* (GenBank: XP_047265719.1). The identified fragments showed 100% sequence identity with the reference sequence and collectively corresponded to 55.9% coverage of the reference protein sequence. The regions corresponding to the identified peptide fragments are highlighted in different colors in Fig. 2, whereas insertions are represented by dashes (-).

3.3 Phylogenetic Analysis of 2S Storage Proteins

Phylogenetic analysis of 2S storage proteins revealed the clustering of sequences according to their evolutionary relatedness within the Solanaceae family (Fig. 3).The proteins from *C. annuum* and *C. galapagoense* formed a single clade,

reflecting the high sequence similarity between species of the genus *Capsicum*. Similarly, the proteins from *Nicotiana tabacum* and *Nicotiana tomentosiformis* clustered together, as expected given the close evolutionary relationship between these species.The *Solanum stenotomum* protein clustered with one of the *Lycium barbarum* sequences (XP_060207128), whereas the second *L. barbarum* sequence (XP_060207129) occupied a distinct position in the phylogenetic tree, suggesting that these proteins represent different members of the 2S albumin family present in this species.Based on sequence similarity to the reference 2S albumin-like protein from *C. annuum*, together with phylogenetic analysis, fraction P1' was identified as a 2S albumin-like protein.

3.4 Hydrodynamic Diameter of P1' Determined by Dynamic Light Scattering

The particle size distribution of P1' showed a profile predominantly characterized by particles with small hydrodynamic diameters (Fig. 4). In the presence of the lipid system composed of POPS/POPC/POPE/Erg and P1'at a concentration of 500 µM, a marked shift toward larger hydrodynamic diameters was observed, with a predominant population in the range of approximately 500–1,000 nm. This increase in the apparent particle size suggests the formation of larger structures, possibly resulting from the association of the protein with the lipid components and/or the formation of protein–lipid complexes. Overall, the presence of the lipid system significantly altered the size distribution profile of P1' in solution.

3.5 Effect of P1' on the Growth of *C. albicans* and *C. tropicalis*

For *C. albicans*, the IC_{50} values were estimated to range from 6.25 to 3.12 µg·mL^{-1} (Fig. 5A). For *C. tropicalis*, the IC_{50} values were estimated to range from 12.5 to 6.25 µg·mL^{-1} (Fig. 5B). Among the values obtained, an IC_{50} of 6.25 µg·mL^{-1} indicates greater antifungal activity, as a lower concentration of the fraction was required to achieve 50% inhibition of growth. Comparatively, the lower IC_{50} values observed for *C. tropicalis* suggest greater sensitivity of this species to the P1' fraction than *C. albicans* under the conditions evaluated.

3.6 Evaluation of Cell Membrane Permeabilization (SYTOX Green)

To assess whether the inhibitory activity of P1' against the growth of *C. albicans* and *C. tropicalis* was associated with alterations in plasma membrane integrity, concentrations based on the previously determined IC_{50} values were used. For *C. albicans*, no significant fluorescence was detected after treatment with the P1' fraction, indicating the absence of detectable plasma membrane permeabilization under the conditions evaluated. For *C. tropicalis*, as shown in Fig. 6, localized fluorescence was observed after treatment with P1' at a concentration of 6.25 $\mu g \cdot mL^{-1}$, whereas no significant fluorescence was observed at 12.5 $\mu g \cdot mL^{-1}$.

3.7 Evaluation of Reactive Oxygen Species Production

The production of reactive oxygen species (ROS) in *Candida* cells was evaluated by fluorescence microscopy using the H_2DCFDA probe, employing P1' concentrations close to the previously determined IC_{50} values for each species (Fig. 6). For *C. albicans*, no detectable fluorescence was observed following H_2DCFDA staining, indicating no evidence of a significant increase in ROS production under the conditions evaluated. In *C. tropicalis*, the negative control showed no detectable fluorescence, whereas the positive control, consisting of cells treated with 3% acetic acid, exhibited fluorescence, confirming the functionality of the assay. Following treatment with P1', fluorescence was observed in cells treated with both concentrations, indicating increased ROS production in *C. tropicalis*. The presence of fluorescence under both treatment conditions suggests that P1' may induce oxidative stress in this species.

3.8 Assessment of Mitochondrial Membrane Potential

Analysis of mitochondrial membrane potential using JC-1 staining revealed changes in fluorescence in *C. albicans* (Fig. 7) and *C. tropicalis* (Fig. 8) cells following treatment with P1'. In control cells of both species, higher red fluorescence intensity was observed, which is associated with the formation of JC-1 aggregates and, consequently, the maintenance of a higher mitochondrial membrane potential. In *C. albicans*, treatment with P1' at concentrations of 3.12 and 6.25 µg/mL resulted in a reduction in fluorescence associated with JC-1 aggregates, with this change being more pronounced at 6.25 µg/mL. Similarly, in *C. tropicalis*, cells treated with P1' at concentrations of 6.25 and 12.5 µg/mL showed reduced red fluorescence

and a relative increase in green fluorescence, corresponding to the monomeric form of the dye. Thus, a reduction in mitochondrial membrane potential occurred in both species following treatment with P1', suggesting mitochondrial depolarization, although different response patterns were observed under the conditions evaluated.

3.9 Structural Modeling of the P1' 2S Albumin-Like Protein

The three peptide fragments identified in P1' showed sequence similarity to regions of 2S albumin-like proteins. Among the retrieved candidates, the hypothetical protein P3S67_003004 from *Capsicum chacoense* (KAM3321853.1) was identified as a potential match. Sequence alignment revealed 100% identity for two peptide fragments and 94.12% identity for the third with the candidate protein (Fig. 9A).

The structural model generated using SWISS-MODEL exhibited a predominantly α-helical architecture, consistent with the characteristic fold of 2S albumins. Structural alignment with the experimentally determined 2S albumin Ara h 6 (PDB ID: 8SJA, chain D) allowed the corresponding 2S albumin-like structural domain to be delineated. Mapping of the three experimentally identified peptides onto the resulting model revealed their localization within this structural domain (Fig. 9B), further supporting the presence of a 2S albumin-like protein in P1'.

3.10 Molecular Docking with Representative Fungal Cell Wall and Membrane Components

Molecular docking was used to explore potential interactions between the modeled 2S albumin-like candidate and selected fungal cell-envelope components. The predicted binding affinity energies ranged from −7.114 to −9.195 kcal mol^{-1} (Table 1). Among the tested ligands, 6-O-glucosyl-laminaritriose showed the most negative predicted affinity energy (−9.195 kcal mol^{-1}), followed by ergosterol (−9.006 kcal mol^{-1}), $GlcNAc_4$ (−8.736 kcal mol^{-1}), laminaritriose (−8.064 kcal mol^{-1}), and Man_2 (−7.114 kcal mol^{-1}). These values represent computational predictions .

The predicted interaction profiles differed among the ligands. For $GlcNAc_4$, PLIP identified predominantly hydrogen-bond interactions involving Ser1, Cys2, Gln3, Gln4, Arg58, Gln62, and Gln66 (Fig. 10A; Table 1; Supplementary Table S1). The

complex with laminaritriose also showed predominantly hydrogen-bond interactions involving Ser1, Cys2, Gln3, Arg58, Gln59, and Gln62, together with a predicted salt bridge involving Arg58 (Fig. 10C; Table 1; Supplementary Table S1). For Man_2, five hydrogen-bond interactions were predicted, involving Ser1, Cys2, Gln3, and Gln4 (Fig. 10D; Table 1; Supplementary Table S1). The complex with 6-O-glucosyl-laminaritriose presented the largest number of predicted contacts, including hydrogen bonds involving Tyr18, Arg22, Arg34, Arg73, Gln77, Gln80, Gln83, Asn84, and Arg95, as well as a predicted salt bridge involving Arg22 (Fig. 10E; Table 1; Supplementary Table S1).

In contrast, the predicted ergosterol complex involved four hydrophobic contacts associated with Gln51 and Pro93, with no hydrogen bonds or salt bridges detected by PLIP (Fig. 10B; Table 1; Supplementary Table S1). This limited interaction profile does not provide sufficient evidence to infer specific or biologically relevant binding to ergosterol. Overall, the docking results identify possible interaction modes for further investigation, particularly with the selected carbohydrate ligands, but do not establish direct binding or a functional mechanism.

4. Discussion

The genus *Capsicum* constitutes a relevant source of antimicrobial proteins and peptides associated with plant defense, including molecules belonging to different protein families [11]. Among these proteins, 2S albumins, traditionally associated with nutrient storage, have also been linked to antimicrobial activities [34]. In *C. annuum*, two proteins homologous to 2S albumins have previously been characterized and shown antifungal activity against pathogenic fungi [18], indicating that this protein family may perform functions beyond storage. Thus, the identification of P1' in *C. chinense* seeds expands the knowledge of the occurrence of 2S albumin-like proteins in *Capsicum* and, together with the antifungal activity observed in the present study, reinforces the potential of these proteins as components of plant defense.

From the perspective that *C. chinense* seeds have been shown to be an important source of natural peptides with antimicrobial activity, as previously described by [11,12], the present study investigated the antimicrobial potential of a

hydrophilic fraction, designated P1', obtained by reverse-phase chromatography (Fig. 1).

The presence of a well-defined peak during reverse-phase chromatography enabled the selection of fraction P1' for subsequent molecular characterization analyses. Mass spectrometric analysis revealed three peptide fragments showing similarity to the 2S albumin sequence of *C. annuum* (Fig. 2). Comparison of the fragments identified in P1' with the reference sequence revealed 100% conservation of the amino acid residues present in the analyzed fragments, further supporting the association between the protein present in P1' and 2S albumins from *C. annuum*. In addition, four cysteine residues were identified among the three fragments. The conservation of these residues is relevant because 2S albumins are characterized by the presence of highly conserved cysteine residues, generally eight, which participate in the formation of disulfide bonds responsible for stabilizing their three-dimensional structure [8]. Similar patterns of residue conservation have also been observed in 2S albumin fragments identified in other plant species, such as *Lycopersicon esculentum*, *Cannabis sativa*, *Nelumbo nucifera*, and pomegranate, further highlighting the importance of these residues for maintaining the structural characteristics of this protein family [8, 19, 20, 21]. Therefore, the conservation observed in the P1' fragments provides relevant evidence for the assignment of homologous proteins, particularly when combined with similarity analyses against protein databases. In addition, the approximately 40% sequence coverage of the reference protein provides further support for the molecular identification and suggests conservation of these regions among 2S proteins of the genus *Capsicum*.

Structural modeling complemented the identification of the protein fragments and provided additional support for their association with a 2S albumin-like protein. The predominance of α-helices in the model and the positioning of the fragments within the conserved structural core of this protein family are consistent with the organization described for 2S albumins, which are characterized by a helical scaffold stabilized by disulfide bonds [5, 22, 23]. This structural conservation is particularly relevant because proteins of the 2S family may exhibit differences in their primary sequences while retaining conserved structural features [24, 25].

Thus, the modeling data strengthen the structural assignment of the fragments, although they do not allow the identity of the functional protein to be established.

Phylogenetic analysis of 2S storage proteins complements the evidence obtained by mass spectrometric analysis of the fragments and provides an evolutionary context for this assignment within the Solanaceae family (Fig. 3). The sequences of *C. annuum* (XP_047265719) and *C. galapagoense* (KAM3343852) clustered within the same clade, consistent with the evolutionary proximity between these species and with the high similarity observed between the P1' fragments and the *C. annuum* reference sequence. This proximity is consistent with the conservation of structural features of 2S albumins, including cysteine residues and specific protein regions, despite variations in the primary sequence [19, 26]. In this context, the high similarity between the P1' fragments and the *C. annuum* sequence, together with the clustering of *Capsicum* proteins, further supports their association with the 2S albumin family without implying identity between the complete protein sequences [25].

The clustering of the *N. tabacum* (XP_075101966) and *N. tomentosiformis* (XP_009590596) proteins also reflected the evolutionary proximity between related species. Conversely, the position of *S. stenotomum* (XP_049377253) close to one of the *L. barbarum* sequences (XP_060207129), whereas the *L. barbarum* sequence XP_060207128 occupied a distinct position, highlights the diversity among members of the 2S family. This pattern may be related to the multigenic nature of storage proteins, which allows the occurrence of different homologous members within the same species [27, 28]. Overall, the observed clustering patterns, particularly among *Capsicum* species, together with the structural conservation of 2S proteins, especially in the C-terminal region where the fragments identified in P1' are located, provide additional evidence supporting the assignment of fraction P1' as a 2S albumin. Therefore, this 2S albumin-enriched fraction from *C. chinense* will hereafter be referred to as P1'.

Following the identification and characterization of P1', its structural behavior in solution was investigated by determining its hydrodynamic diameter in the absence and presence of a lipid system composed of POPS/POPC/POPE/ergosterol (Fig. 4). This analysis allows potential changes in the dispersion state of the protein to

be assessed and provides insights into its interaction with lipid components, which is particularly relevant when considering the interaction of antimicrobial proteins with membrane lipids. The absence of large particles in the sample containing P1' alone suggests that, under the conditions evaluated, the fraction remains predominantly dispersed in solution and shows no evidence of the formation of larger aggregates detectable by DLS [29].

In contrast, the change observed after addition of the lipid system indicates that the membrane environment influences the behavior of the fraction. This difference is relevant because it suggests that the formation of larger structures is associated with the presence of lipids rather than exclusively with spontaneous self-aggregation of P1'. In peptide–membrane systems, changes in hydrodynamic diameter may result from aggregation, vesicle approximation or interconnection, membrane reorganization, or the formation of supramolecular structures induced by interaction with the analyzed molecule [30, 31, 32]. Therefore, the behavior observed for P1' indicates a lipid environment-dependent response, although the specific nature of this process cannot be determined solely by DLS.

The composition of the system used should also be considered when interpreting these results. The presence of POPS, an anionic phospholipid, makes a contribution of electrostatic interactions to the association of P1' with lipid structures plausible. Interactions between bioactive molecules and anionic lipids constitute an important mechanism of membrane recognition and may favor association with the surface of negatively charged bilayers compared with systems composed predominantly of zwitterionic lipids [33, 34]. However, protein–membrane interactions are not determined exclusively by surface charge. The presence of POPE may influence bilayer curvature and organization, whereas ergosterol may alter membrane ordering and packing. Thus, the response observed for P1' likely results from a combination of the physicochemical properties of the different components of the system rather than from a single specific interaction [35].

Therefore, the increase in hydrodynamic diameter may reflect different forms of lipid system reorganization. Association of P1' with the surface of the structures could promote particle approximation, while protein–lipid interactions could also

contribute to vesicle clustering or fusion, bilayer reorganization, or the formation of larger supramolecular structures. Similar phenomena have been described for different bioactive peptides, in which membrane interactions may involve multiple events dependent on concentration, molecule-to-lipid ratio, membrane composition, and the tendency toward self-association [31, 36, 37].

The relevance of this finding is related to the antimicrobial potential of P1', since membrane interaction has been described as a component of different mechanisms of action of antimicrobial proteins and peptides. However, such interaction does not necessarily imply pore formation or immediate bilayer disruption and may instead involve alterations in membrane organization, aggregation, lipid-domain formation, or different forms of permeabilization [27, 29, 38].

In addition to their storage function, 2S albumins may exhibit antifungal and antibacterial activities [5,39]. In this context, P1' inhibited the growth of *C. albicans* and *C. tropicalis*, exhibiting different IC_{50} values. Studies of different antimicrobial proteins have demonstrated activity against *Candida* species at concentrations similar to those observed for P1', including compounds with inhibitory concentrations ranging from 3.9 to 15.6 $\mu g \cdot mL^{-1}$ and others ranging from 4 to 32 $\mu g \cdot mL^{-1}$ [40, 41]. Differences in susceptibility among *Candida* species have also been described for different antifungal peptides, including cases of greater activity against *C. tropicalis*, similar responses between species, and marked differences in sensitivity among species and isolates [40, 41, 42, 43, 44]. Thus, the apparently greater sensitivity of *C. albicans* observed in the present study should be interpreted as a specific characteristic of the interaction between P1' and the cells evaluated rather than as a general property of antifungal proteins or peptides.

The antimicrobial activity of plant proteins and peptides may be associated with different mechanisms, including alterations in membrane organization, disruption of intracellular homeostasis, and induction of processes related to oxidative stress [45]. In this context, the inhibitory activity observed for P1' provides evidence of its antifungal potential but, by itself, does not establish the mechanism responsible for this effect. Therefore, alterations in plasma membrane integrity, reactive oxygen species production, and mitochondrial membrane potential were investigated to identify cellular events associated with exposure to the fraction [46,47].

Assessment of membrane integrity using SYTOX Green provided additional evidence regarding the mechanism of action of P1', since this probe enables the detection of plasma membrane permeabilization in cells with compromised membrane integrity [48]. In *C. tropicalis*, fluorescence was observed in some cells following treatment with 6.25 μg·mL^{-1}, whereas no significant signal was detected at 12.5 μg·mL^{-1}. This pattern indicates that probe-detectable permeabilization did not occur in a directly concentration-dependent manner under the conditions evaluated. Similarly, studies with the antifungal protein from *Aspergillus giganteus* demonstrated that permeabilization detected by SYTOX Green occurred only at concentrations above the MIC, highlighting that this assay may have limited sensitivity for detecting certain cellular alterations [49].

The absence of significant fluorescence in *C. albicans*, even at concentrations close to the respective IC_{50} values, further supports the possibility that the antifungal activity of P1' does not depend exclusively on membrane permeabilization. Previous studies have also demonstrated that reductions in cell viability may occur without generalized permeabilization detectable by membrane integrity markers [50].

In plant-derived antimicrobial proteins, association with the cell surface may cause alterations in membrane organization or function without necessarily resulting in pore formation or immediate bilayer disruption [51, 52]. Thus, the results obtained with SYTOX Green indicate that growth inhibition by P1' should not be attributed simply to cell lysis resulting from generalized loss of membrane integrity. The weak fluorescence observed in *C. tropicalis* under one of the conditions evaluated also suggests that membrane alterations, when present, may depend on both species and concentration.

The ROS results provide additional evidence of alterations in intracellular homeostasis associated with the antifungal activity of P1'. In *C. tropicalis*, treatment indicated an increase in reactive oxygen species, suggesting the occurrence of redox imbalance. The involvement of ROS in antifungal activity has been described for different antimicrobial peptides and may be associated with disruption of cellular homeostasis and impairment of processes essential for fungal survival [53]. However, ROS detection does not establish whether oxidative stress represents a

primary or secondary event in the action of P1', since antifungal mechanisms may involve concomitant alterations in membrane integrity, redox homeostasis, and mitochondrial function [54, 55].

In contrast, *C. albicans* showed no detectable ROS fluorescence despite exhibiting apparently greater sensitivity to P1'. This finding indicates that antifungal activity does not necessarily depend on the induction of detectable ROS under the experimental conditions evaluated. Differences in the responses of *Candida* species to antifungal peptides have previously been described and may reflect species-specific characteristics [40, 41, 43]. Thus, the data suggest that P1' may trigger distinct cellular responses, with oxidative stress potentially contributing to its activity against *C. tropicalis*, whereas different mechanisms may contribute to the inhibition of *C. albicans*.

JC-1 analysis indicated an alteration in mitochondrial membrane potential in *C. tropicalis* following treatment with P1', characterized by a reduction in red fluorescence and an increase in green fluorescence, a pattern consistent with mitochondrial depolarization [40, 56, 57]. Together with the increase in ROS and the absence of generalized permeabilization detected by SYTOX Green, these results suggest that the antifungal activity of P1' may involve oxidative stress associated with impaired mitochondrial function rather than predominantly depending on plasma membrane lysis. However, the observed depolarization does not establish the mitochondria as the primary target, since mitochondrial alterations may also occur secondarily to other cellular events [58, 59]. The absence of detectable ROS in *C. albicans* further supports the possibility of species-specific mechanisms underlying the response to P1'.

From this perspective, molecular docking was used to explore potential interactions between the modeled 2S albumin-like candidate associated with the peptide fragments identified in fraction P1' and components of the fungal cell envelope. The predicted interactions with carbohydrate ligands associated with chitin and β-glucans, particularly $GlcNAc_4$, laminaritriose, and 6-O-glucosyl-laminaritriose, involved hydrogen bonds and, in some cases, a predicted salt bridge. Among the tested ligands, 6-O-glucosyl-laminaritriose showed the most negative predicted binding affinity energy and the largest number of predicted contacts.

These findings suggest possible interactions with fungal cell-wall carbohydrates that warrant further investigation. Chitin, β-glucans, and ergosterol are relevant structures for fungal cell integrity and organization and therefore represent biologically plausible targets for molecules with antifungal activity [60, 61, 62]. However, the docking results are predictive and do not demonstrate direct binding or establish the biological relevance of these interactions. In contrast to the carbohydrate ligands, the predicted interaction with ergosterol involved only four hydrophobic contacts associated with Gln51 and Pro93, with no hydrogen bonds or salt bridges detected. Therefore, the available results do not provide sufficient evidence to support specific or biologically relevant binding to ergosterol. Overall, the docking analysis provides hypotheses for future experimental investigation rather than evidence of a confirmed molecular mechanism. Furthermore, because the analysis was based on a modeled candidate and the antifungal activity was measured for fraction P1', these predictions cannot establish that the candidate protein is responsible for the observed activity.

Integration of the results enabled the identification and characterization of a novel 2S albumin-like protein in *C. chinense* seeds (P1'), contributing to the understanding of storage proteins in this species. The antifungal activity observed against *C. albicans* and *C. tropicalis*, species of clinical relevance and included among the fungal pathogens prioritized by the World Health Organization, further highlights the biological potential of P1'. In addition, the investigation of different aspects associated with fungal growth inhibition, including alterations in lipid system organization and assessment of membrane integrity, provides initial evidence regarding its possible mode of action. Considering that this is, to date, the first report of a 2S albumin-like protein with characterized antifungal activity in *C. chinense*, these findings expand current knowledge of the functional potential of seed proteins from this species and provide a basis for further investigations into their molecular mechanisms and biotechnological potential.

5. Conclusion

In summary, P1' is a 2S albumin-like protein from *C. chinense* seeds that exhibits significant antifungal activity against *C. albicans* and *C. tropicalis*. The results demonstrate that this seed storage protein possesses biological activity

beyond its classic nutritional function and provide initial insights into its potential interaction with fungal cells. Thus, P1' expands the repertoire of bioactive proteins identified in *Capsicum* and represents a promising target for future studies on plant-derived antifungal compounds.

Acknowledgments: This work was performed at the Universidade Estadual do Norte Fluminense Darcy Ribeiro (UENF). We wish to thank L.C.D. Souza and V.M. Kokis for technical assistance.

Funding This work was performed at the Universidade Estadual do Norte Fluminense Darcy Ribeiro (UENF). We wish to thank L.C.D. Souza and V.M. Kokis for technical assistance. We acknowledge the financial support of the Brazilian agencies Conselho Nacional de Desenvolvimento Científico e Tecnológico − CNPq (403302/2023-4; 301094/2026-8; 302966/2026-9, 307590/2021-6; 312339/2025-9; 406990/2025-5; 306429/2023-3), Fundação Carlos Chagas Filho de Amparo à Pesquisa do Estado do Rio de Janeiro − FAPERJ (E-26/210.353/2022; E-26/200.127/2023; E-26/204.312/2025; E-26/210.563/2026; E-26/210.746/2025; E-26/200.180/2026; E-26/200.177/2023; E-26/204.310/2025, E-26/203.948/2024), PAPIC UENF (SEI-260.002/007059/2024; SEI-260.002/007048/2024; SEI-260002/007051/2024) and Financiadora de Estudos e Projetos (FINEP) under the FINEP/MCTI/FNDCT/PROINFRA 2021 program (Agreement No. 0.1.22.0442.00). This study was also financed in part by the Coordenação de Aperfeiçoamento de Pessoal de Nível Superior − Brasil (CAPES), finance code 001.

Data Availability: All data generated or analysed during this study are included in this published article.

Conflict of Interest: The authors declare no conflict of interest

Ethical Approval This article does not contain any studies with human or animal subjects.

Author contribution

The study was conceived by VMG and APBFO. Experimental procedures were carried out by APBFO,GMP, LMR, MPCMS, SRF and LYMS. Data analyses were performed by AEAO, AOC and AEZ. The paper was written and revised by LMR, VMG, GBT and EOM. All authors reviewed the manuscript.

6. References

1. Artur MAS, Kajala K (2021) Convergent evolution of gene regulatory networks underlying plant adaptations to dry environments. Plant Cell Environ 44:3211–3222

2. Becker A, Chen X, Dresselhaus T, Gutsche N, Müller-Schüssele SJ, Sprunck S, Theißen G, de Vries S, Zachgo S (2025) Sexual reproduction in land plants: an evolutionary perspective. Plant Reprod 38:12

3. Kozaki A, Aoyanagi T (2022) Molecular aspects of seed development controlled by gibberellins and abscisic acids. Int J Mol Sci 23:1876

4. Yang T, Wu X, Wang W, Wu Y (2023) Regulation of seed storage protein synthesis in monocot and dicot plants: a comparative review. Mol Plant 16:145–167

5. Souza PFN (2020) The forgotten 2S albumin proteins: importance, structure, and biotechnological application in agriculture and human health. Int J Biol Macromol 164:4638–4649

6. Adewole TS, Dudu BB, Oladele JO, Oyeleke OM, Kuku A (2023) Functional bioactivities of soluble seed proteins from two leguminous seeds. Prev Nutr Food Sci 28:160–169

7. Jain A (2023) Seed storage protein, functional diversity and association with allergy. Allergies 3:25–38

8. Tuppo L, Alessandri C, Zaccaro L, Giangrieco I, Tamburrini M, Mari A, Ciardiello MA (2024) Isolation, characterization and IgE binding of two 2S albumins of pomegranate seeds. Foods 13:1965

9. Madage VA, Dongare PM, Deshpande NV, Giri AP, Pawar PK (2025) The 2S albumin-like protein from *Amaranthus* disrupts insect metabolism and triggers antibiosis. Pest Manag Sci 81:8367–8382

10. Fisher MC, Gurr SJ, Cuomo CA, Blehert DS, Jin H, Stukenbrock EH, Stajich JE, Kahmann R, Boone C, Denning DW, Gow NAR, Klein BS, Kronstad JW, Sheppard DC, Taylor JW, Wright GD, Heitman J, Casadevall A, Cowen LE (2020) Threats

790 posed by the fungal kingdom to humans, wildlife, and agriculture. mBio 11:e00449-
791 20

792 11. Oliveira APBF, Resende LM, Rodrigues R, de Oliveira Mello E, Taveira GB, de
793 Oliveira Carvalho AO, Gomes VM (2022) Antimicrobial peptides of the genus
794 Capsicum: a mini review. Hortic Environ Biotechnol 63:453–466

795 12. Oliveira APBF, Resende LM, da Silva MS, dos Santos LA, Carvalho AO,
796 Chaves RP, Nagano CS, Moreira FF, Seabra SH, da Cunha M, de Oliveira ÉM,
797 Taveira GB, Rodrigues R, Gomes VM (2025) Lipid transfer proteins (LTPs) partially
798 purified from *Capsicum chinense* Jacq. seeds: antifungal properties and α-amylase
799 inhibitory activity. Protein J 44:201–212

800 13. Broekaert WF, Terras FRG, Cammue BPA, Vanderleyden J (1990) An
801 automated quantitative assay for fungal growth inhibition. FEMS Microbiol Lett
802 69:55–59

803 14. Thevissen K, Terras FR, Broekaert WF (1999) Permeabilization of fungal
804 membranes by plant defensins inhibits fungal growth. Appl Environ Microbiol
805 65:5451–5458

806 15. Mello EO, Ribeiro SF, Carvalho AO, Santos IS, da Cunha M, Santa-Catarina C,
807 Gomes VM (2011) Antifungal activity of PvD1 defensin involves plasma membrane
808 permeabilization, inhibition of medium acidification, and induction of ROS in fungi
809 cells. Curr Microbiol 62:1209–1217

810 16. Yan T, An L, Chen F (2022) Recombinant phage displaying ToAP2D peptide
811 with antifungal activity against Sporothrix globosa. Front Pharmacol 13:1022651

812 17. Adasme MF, Linnemann KL, Bolz SN, Kaiser F, Salentin S, Haupt VJ,
813 Schroeder M (2021) PLIP 2021: expanding the scope of the protein–ligand
814 interaction profiler to DNA and RNA. Nucleic Acids Res 49:W530–W534

815 18. Ribeiro SFF, Taveira GB, Carvalho AO, Santos IS, da Cunha M, Santa-Catarina
816 C, Gomes VM (2012) Antifungal and other biological activities of two 2S albumin-
817 homologous proteins against pathogenic fungi. Protein J 31:59–67

19. Sun X, Sun Y, Li Y, Wu Q, Wang L (2021) Identification and characterization of the seed storage proteins and related genes of *Cannabis sativa* L. Front Nutr 8:678421

20. Oguri S, Kamoshida M, Nagata Y, Momonoki YS, Kamimura H (2003) Characterization and sequence of tomato 2S seed albumin: a storage protein with sequence similarities to the fruit lectin. Planta 216:976–984

21. Khan S, Ali SA, Yasmin T, Ahmed M, Khan H (2016) Purification and characterization of 2S albumin from *Nelumbo nucifera*. Biosci Biotechnol Biochem 80:2109–2114

22. Pantoja-Uceda D, Bruix M, Giménez-Gallego G, Rico M, Santoro J (2003) Solution structure of RicC3, a 2S albumin storage protein from *Ricinus communis*. Biochemistry 42:13839–13847

23. Ullah A, Mariutti R, Masood R, Caruso Í, Costa G, Santos CR, Zanphorlin L, Murakami M, Arni R (2015) Crystal structure of mature 2S albumin from *Moringa oleifera* seeds. Biochem Biophys Res Commun 468:365–371

24. Freire JEC, Vasconcelos IM, Moreno FB, Batista AB, Lobo M, Pereira ML, Lima JP, Almeida RVM, Sousa AJS, Monteiro-Moreira A, Oliveira J, Grangeiro TB (2015) Mo-CBP3, an antifungal chitin-binding protein from Moringa oleifera seeds, is a member of the 2S albumin family. PLoS One 10:e0119871

25. Yadav A, Jaiswal P, Mathew IE, Panwar A, Agarwal P (2026) Decoding rice seed storage proteins: from gene identification to structural prediction. Ann Bot (2026):mcag124

26. Zhang W, Xu J, Bennetzen JL, Messing J (2016) Teff, an orphan cereal in the Chloridoideae, provides insights into the evolution of storage proteins in grasses. Genome Biol Evol 8:1712–1721

27. Li C, Li M, Dunwell JM, Zhang YM (2012) Gene duplication and an accelerated evolutionary rate in 11S globulin genes are associated with higher protein synthesis in dicots as compared to monocots. BMC Evol Biol 12:15

28. Artur MAS, Zhao T, Ligterink W, Schranz E, Hilhorst HWM (2019) Dissecting the genomic diversification of late embryogenesis abundant (LEA) protein gene families in plants. Genome Biol Evol 11:459–471

29. Larionova OS, Drevko YB, Khanadeev VA, Gorshunova SV, Kozlov ES, Larionov SV (2023) Analysis of protein fractions of water-soluble peptides by dynamic light scattering. Izv Saratov Univ Phys 23:37–45

30. Kohut G, Juhász T, Quemé-Peña M, Bősze SE, Beke-Somfai T (2021) Controlling peptide function by directed assembly formation: mechanistic insights using multiscale modeling on an antimicrobial peptide–drug–membrane system. ACS Omega 6:15756–15769

31. Manzini MC, Perez KR, Riske KA, Bozelli JC Jr, Santos TL, da Silva MA, Saraiva GKV, Politi MJ, Valente AP, Almeida FCL, Chaimovich H, Rodrigues MA, Bemquerer MP, Schreier S, Cuccovia IM (2014) Peptide–lipid ratio and membrane surface charge determine the mechanism of action of the antimicrobial peptide BP100. Conformational and functional studies. Biochim Biophys Acta Biomembr 1838:1985–1999

32. Furuya ML, Carretero GP, Bemquerer MP, Kiyota S, Rodrigues MA, de Nardi Gaziri TJN, Zuluaga NLB, Matsubara DK, Wandermuren MN, Riske KA, Chaimovich H, Schreier S, Cuccovia IM (2025) Structural and functional effects of the interaction between an antimicrobial peptide and its analogs with model bacterial and erythrocyte membranes. Biomolecules 15:1143

33. Beck K, Nandy J, Hoernke M (2025) Strong membrane permeabilization activity can reduce selectivity of cyclic antimicrobial peptides. J Phys Chem B 129:2446–2460

34. Bozelli JC Jr, Sasahara ET, Pinto MRS, Nakaie CR, Schreier S (2012) Effect of head group and curvature on binding of the antimicrobial peptide tritrpticin to lipid membranes. Chem Phys Lipids 165:365–373

35. Bechinger B, Gorr SU (2017) Antimicrobial peptides: mechanisms of action and resistance. J Dent Res 96:254–260

875 36. Marx L, Semeraro EF, Mandl J, Kremser J, Frewein MP, Malanovic N, Lohner
876 K, Pabst G (2021) Bridging the antimicrobial activity of two lactoferricin derivatives
877 in E. coli and lipid-only membranes. Front Med Technol 3:625975

878 37. Wadhwani P, Reichert J, Bürck J, Ulrich AS (2012) Antimicrobial and cell-
879 penetrating peptides induce lipid vesicle fusion by folding and aggregation. Eur
880 Biophys J 41:177–187

881 38. Gomes IP, Santos TL, de Souza AN, Nunes LO, Cardoso GA, Matos CO, Costa
882 LMF, Lião LM, Resende JM, Verly RM (2021) Membrane interactions of the anuran
883 antimicrobial peptide HSP1-NH2: different aspects of the association to anionic and
884 zwitterionic biomimetic systems. Biochim Biophys Acta Biomembr 1863:183449

885 39. Cândido ES, Pinto MF, Pelegrini PB, Lima TB, Silva ON, Pogue R, Grossi-de-
886 Sá MF, Franco OL (2011) Plant storage proteins with antimicrobial activity: novel
887 insights into plant defense mechanisms. FASEB J 25:3290–3305

888 40. Sun CQ, Peng J, Yang LB, Jiao ZL, Zhou LX, Tao RY, Zhu LJ, Tian ZQ, Huang
889 MJ, Guo G (2022) A cecropin-4 derived peptide C18 inhibits *Candida albicans* by
890 disturbing mitochondrial function. Front Microbiol 13:872322

891 41. Amirrajab N, Amin Ayatollahi Mousavi SA, Taheri B, Salari S, Sarsahra NAA
892 (2023) In vitro antifungal potency of the moronecidin-like peptide against *Candida*
893 *albicans*, *Candida glabrata,* and *Candida tropicalis*. Iran J Microbiol 15:456–461

894 42. Neto JMM, Aguiar TKB, Oliveira MF, Chaves QLSG, Mourão DRAL, Silva VO,
895 Nascimento MTV, Carneiro RF, Martins RX, Farias DF, Sousa BF, Sousa JS,
896 Ramos MV, Freitas CDT (2025) Nicotianin-I: a tobacco floral nectar peptide with
897 anticandidal activity. ACS Omega 10:20213–20225

898 43. Guevara-Lora I, Bras G, Juszczak M, Karkowska-Kuleta J, Gorecki A,
899 Manrique-Moreno M, Dymek J, Pyza E, Kozik A, Rapala-Kozik M (2022) Cecropin
900 D-derived synthetic peptides in the fight against *Candida albicans* cell filamentation
901 and biofilm formation. Front Microbiol 13:1045984

902 44. Paduszynska MA, Neubauer D, Kamysz W, Kamysz E (2025) Anticandidal
903 activity of lipopeptides containing a peptide fragment derived from LL-37, KR12.
904 Molecules 30:1598

905 45. Chiu T, Poucet T, Li YR (2022) The potential of plant proteins as antifungal
906 agents for agricultural applications. Synth Syst Biotechnol 7:1075–1083

907 46. Resende LM, Zeraik AE, Oliveira APBF, Souza TAM, Taveira G, Moreira FF,
908 Seabra S, Ferreira AT, Perales J, Rodrigues R, Gomes VM (2024) Defensin-like
909 peptides from *Capsicum chinense* induce increased ROS, loss of mitochondrial
910 functionality, and reduced growth of the fungus *Colletotrichum scovillei.* Pest Manag
911 Sci

912 47. Taveira G, Machado O, Rodrigues R, Carvalho A, Gomes VM (2019)
913 Characterization and antifungal activity of a plant peptide expressed in the
914 interaction between *Capsicum annuum* fruits and the anthracnose fungus. Biosci
915 Rep

916 48. Mishra SK, Kuppusamy R, Nguyen C, Doeur J, Atwal H, Attard S, Sørensen K,
917 Lin JS, Wong EHH, Hui A, Barron AE, Kumar N, Willcox MDP (2025) Evaluation of
918 the synergistic activity of antimicrobial peptidomimetics or colistin sulphate with
919 conventional antifungals against yeasts of medical importance. J Fungi 11:370

920 49. Theis T, Wedde M, Meyer V, Stahl U (2003) The antifungal protein from
921 Aspergillus giganteus causes membrane permeabilization. Antimicrob Agents
922 Chemother 47:588–593

923 50. Seyedjavadi S, Khani S, Eslamifar A, Ajdary S, Goudarzi M, Halabian R, Akbari
924 R, Zare-Zardini H, Fooladi AII, Amani J, Razzaghi-Abyaneh M (2020) The antifungal
925 peptide MCh-AMP1 derived from Matricaria chamomilla inhibits *Candida albicans*
926 growth via inducing ROS generation and altering fungal cell membrane
927 permeability. Front Microbiol 10:3150

928 51. Teker T, Albayrak G (2026) The Snakin family of antimicrobial peptides:
929 promising alternatives to conventional antibiotics. Pharmaceuticals 19:788

52. Cresca S, Borišek J, Magistrato A, Križaj I (2026) Current status of molecular dynamics simulations of membrane permeabilization by antimicrobial peptides and pore-forming proteins: a review. J Chem Inf Model 66:1982–2005

53. Seyedjavadi SS, Khani S, Eslamifar A, Ajdary S, Goudarzi M, Halabian R, Akbari R, Zare-Zardini H, Imani Fooladi AA, Amani J, Razzaghi-Abyaneh M (2020) The antifungal peptide MCh-AMP1 derived from *Matricaria chamomilla* inhibits *Candida albicans* growth via inducing ROS generation and altering fungal cell membrane permeability. Front Microbiol 10:3150

54. Chang CK, Kao MC, Lan CY (2021) Antimicrobial activity of the peptide LfcinB15 against *Candida albicans*. J Fungi 7:519

55. Vargas-Casanova Y, Bravo-Chaucanés CP, de la Cámara Fuentes S, Martinez-Lopez R, Monteoliva L, Gil C, Rivera-Monroy ZJ, Costa GM, Castañeda JEG, Parra-Giraldo CM (2024) Antifungal synergy: mechanistic insights into the R-1-R peptide and Bidens pilosa extract as potent therapeutics against *Candida* spp. through proteomics. Int J Mol Sci 25:8938

56. Ge A, Zhou H, Yang X, Zhao C, Xin C, Song Z (2025) The antifungal effects of equol against *Candida albicans* involve mitochondrial dysfunction. J Fungi 11:339

57. Costa I, Lopes I, Morais M, Silva R, Remião F, Medeiros R, Alves LG, Pinto E, Cerqueira F (2024) Disclosing the antifungal mechanisms of the cyclam salt H4[H2(4-CF3PhCH2)2Cyclam]Cl4 against *Candida albicans* and *Candida krusei*. Int J Mol Sci 25:5209

58. Kim S, Lee DG (2019) Role of calcium in reactive oxygen species-induced apoptosis in *Candida albicans*: an antifungal mechanism of antimicrobial peptide PMAP-23. Free Radic Res 53:8–17

59. Muñoz-Megías ML, Sánchez-Fresneda R, Solano F, Maicas S, Martínez-Esparza M, Argüelles J (2023) Itraconazole-induced antifungal effect in *Candida parapsilosis* depends largely on oxidative stress generated in mitochondria. Curr Genet 69:165–173

60. Zhao F, Li Q, Wu H, Huang JD, Ju JQ (2022) Synergistic antifungal mechanism of effective components from essential oil against *Penicillium roqueforti*. Eng Microbiol 3:100057

61. Ju J, Guo Y, Cheng Y, Yao W (2022) Analysis of the synergistic antifungal mechanism of small molecular combinations of essential oils at the molecular level. Ind Crops Prod:115612

62. Khoza TG, Dubery I, Piater L (2019) Identification of candidate ergosterol-responsive proteins associated with the plasma membrane of *Arabidopsis thaliana*. Int J Mol Sci 20:1302

7. Images

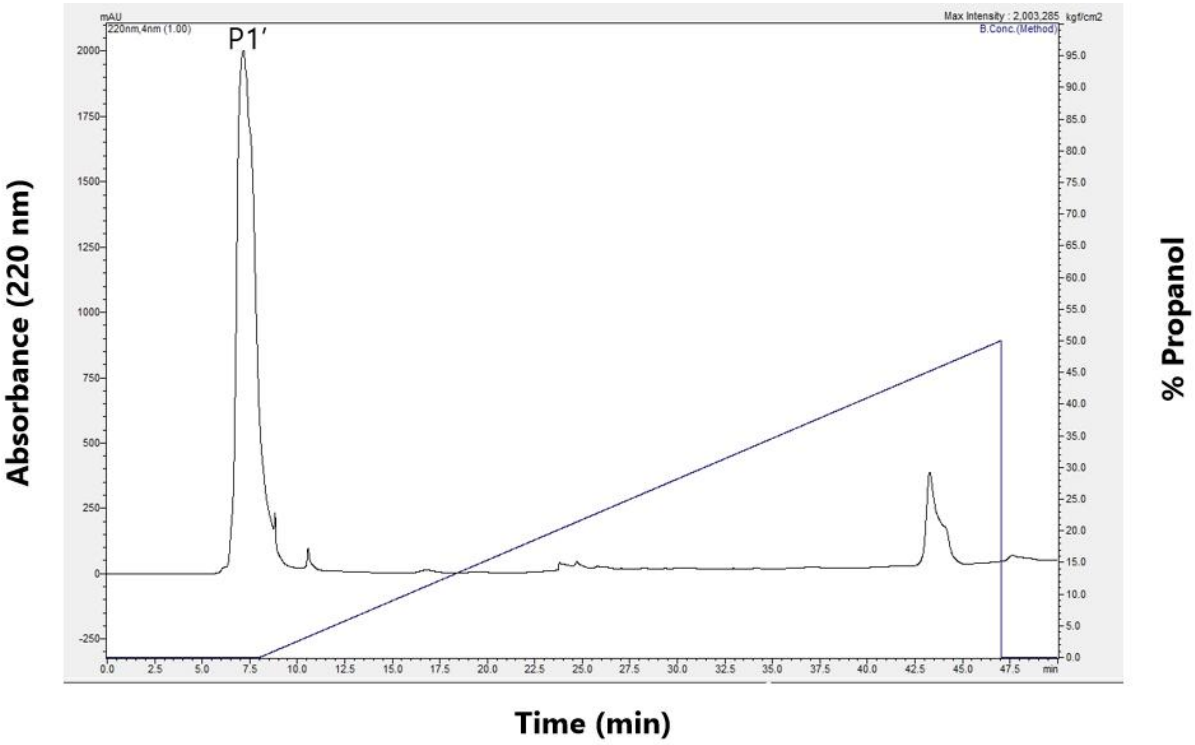

Fig. 1. Chromatographic profile of fraction P1' obtained by reversed-phase chromatography on a µRP-C18 column, monitored at 220 nm. The column was pre-equilibrated with 0.1% TFA (solvent A), and sample elution was performed using a linear gradient of propanol (solvent B) at a flow rate of 0.5 mL min^{-1}.

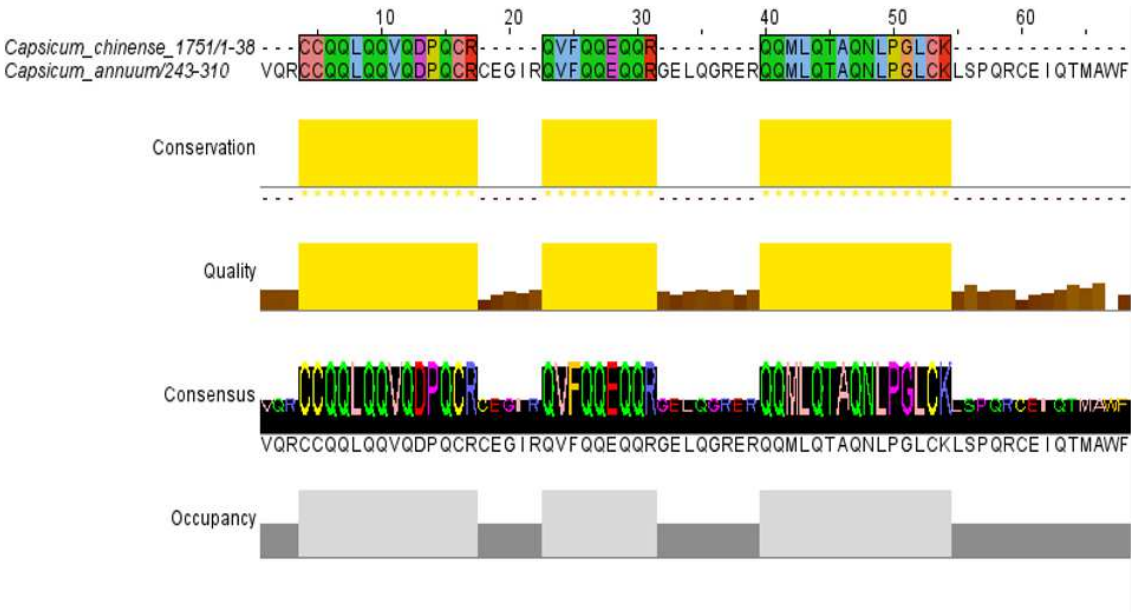

Fig. 2. Multiple sequence alignment of the amino acid sequence of fraction P1' from *Capsicum chinense* seeds (UENF accession 1751) with homologous sequences identified by BLAST. The sequences were aligned using Clustal Omega and visualized with Jalview. Identical residues are highlighted according to the Clustal. Gaps (-) were introduced to optimize the alignment and preserve the correspondence between homologous regions. The Conservation, Quality, Consensus, and Occupancy profiles are shown below the alignment.

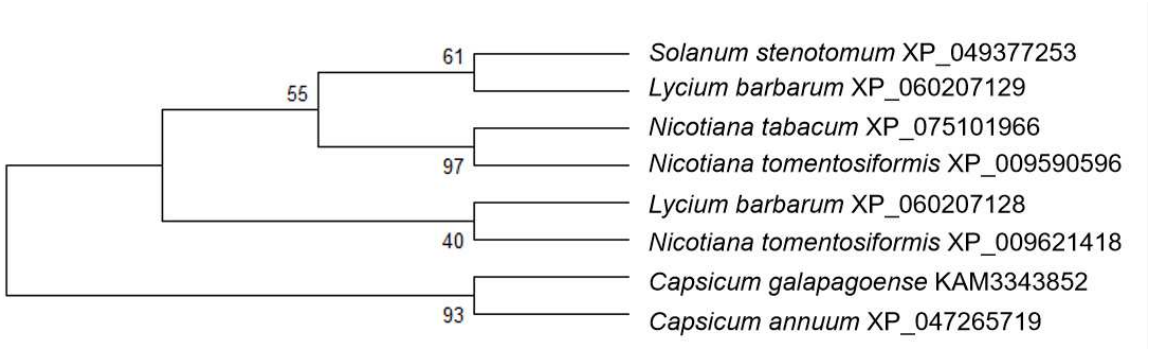

Fig. 3. Phylogenetic tree of 2S albumin-type seed storage proteins from species of the Solanaceae family, reconstructed by the Maximum Likelihood method using the cpREV+G+F model. The analysis was based on orthologous sequences of complete proteins, and branch support values were obtained from 1000 bootstrap pseudoreplicates.

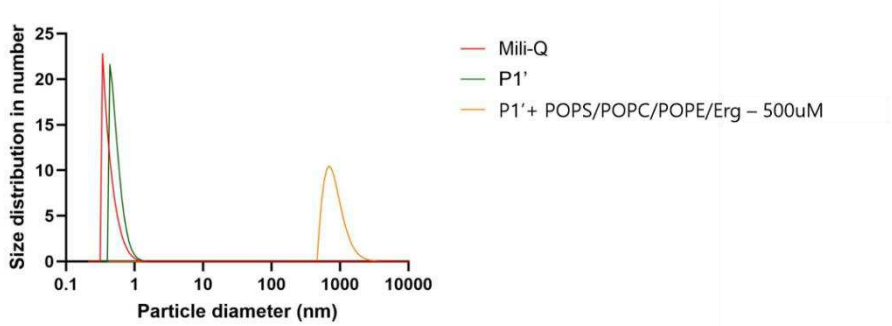

Fig. 4. Particle size distribution determined by dynamic light scattering (DLS) for Milli-Q water (control), P1', and P1' in the presence of the lipid compound POPS/POPC/POPE/ergosterol (500 μM). The hydrodynamic diameter distribution profiles obtained for each sample are shown.

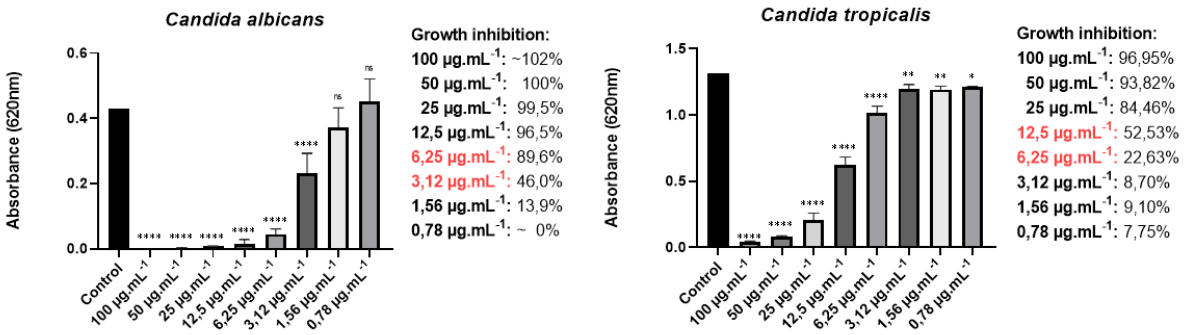

Fig.5. Antifungal activity of P1', obtained via HPLC from *C.chinense* seeds (accession 1751), against the growth of *C. tropicalis* and *C. albicans.* Fungal growth was assessed by measuring absorbance at 620 nm after 24 h of incubation with different concentrations of fraction P1' (0.78–100 µg·mL⁻¹). Data represent the mean ± standard deviation of three independent experiments. Concentrations highlighted in red correspond to the ranges used to determine the IC_{50} for each species.

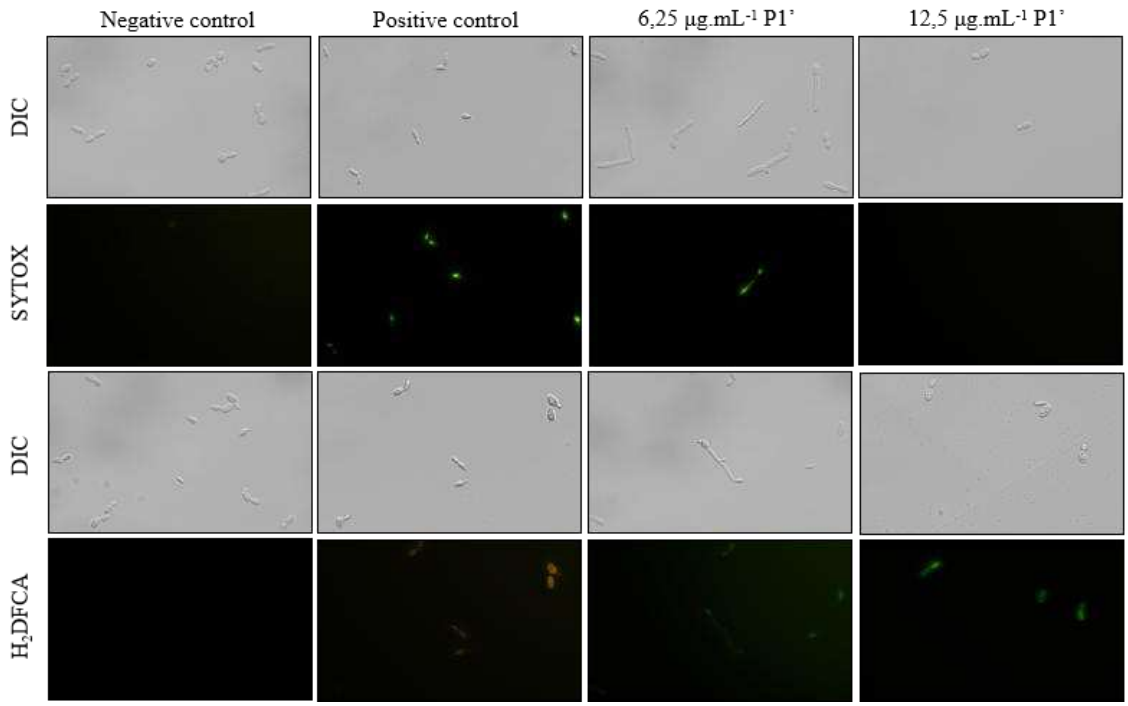

Fig. 6. Evluation of plasma membrane permeabilization and reactive oxygen species (ROS) generation in *C. tropicalis* treated with P1'. Representative DIC and fluorescence microscopy images of untreated cells, used as the negative control; heat-treated cells at 100 °C, used as the positive control for plasma membrane permeabilization; cells treated with 3% acetic acid, used as the positive control for ROS generation; and cells treated with 6.25 and 12.5 µg·mL^{-1} D-CDF-GK for 15 h. For plasma membrane permeabilization analysis, cells were stained with SYTOX Green, whereas ROS generation was assessed using H_2DCFDA. Scale bars = 20 µm.

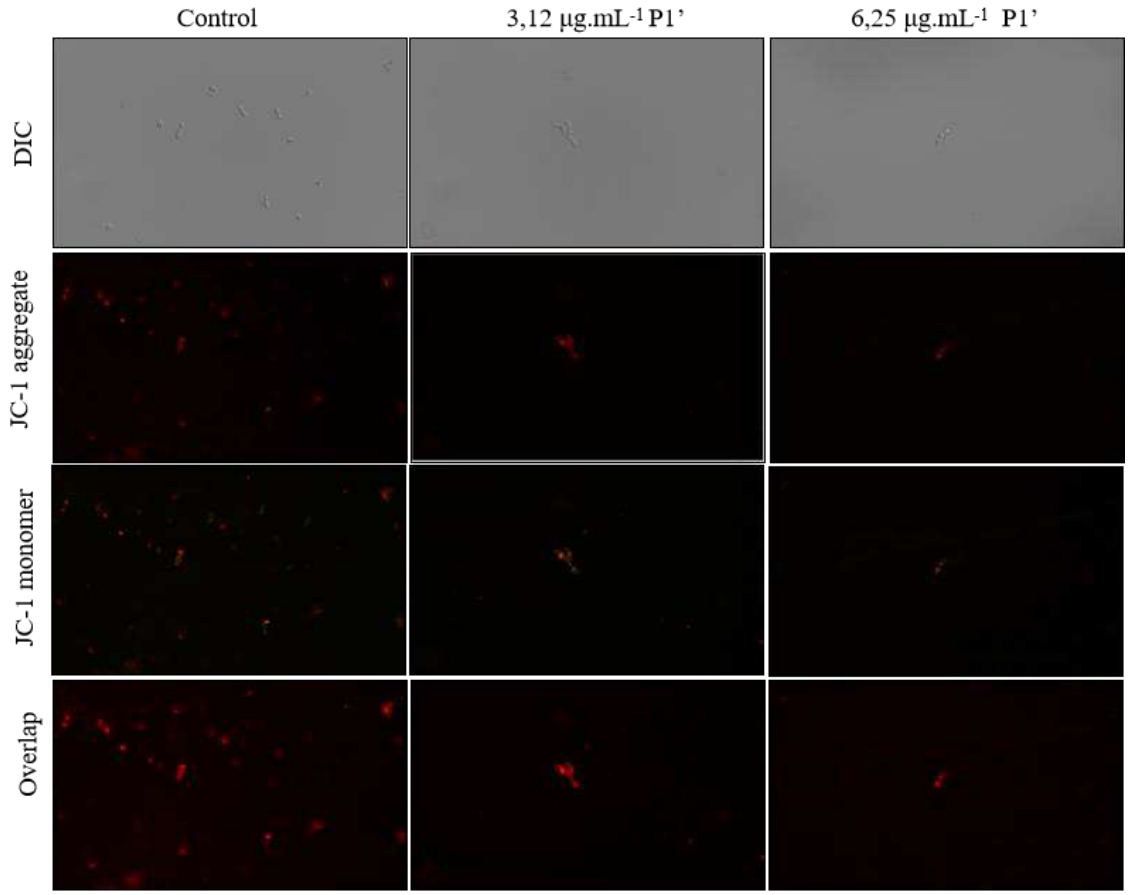

Fig. 7. Assessment of mitochondrial functionality in *C. albicans* after treatment with D-CDF-GK. Representative DIC and fluorescence microscopy images of yeast-phase *C. albicans* cells treated with 3,12 µg.mL-1 and 6,25 µg.mL-1 D-CDF-GK for 15 h and stained with JC-1. Untreated cells stained with JC-1 were used as the control. D-CDF-GK-treated cells showed reduced red fluorescence and a predominance of green fluorescence, indicating decreased mitochondrial membrane potential compared with untreated cells. Scale bars = 10 µm.

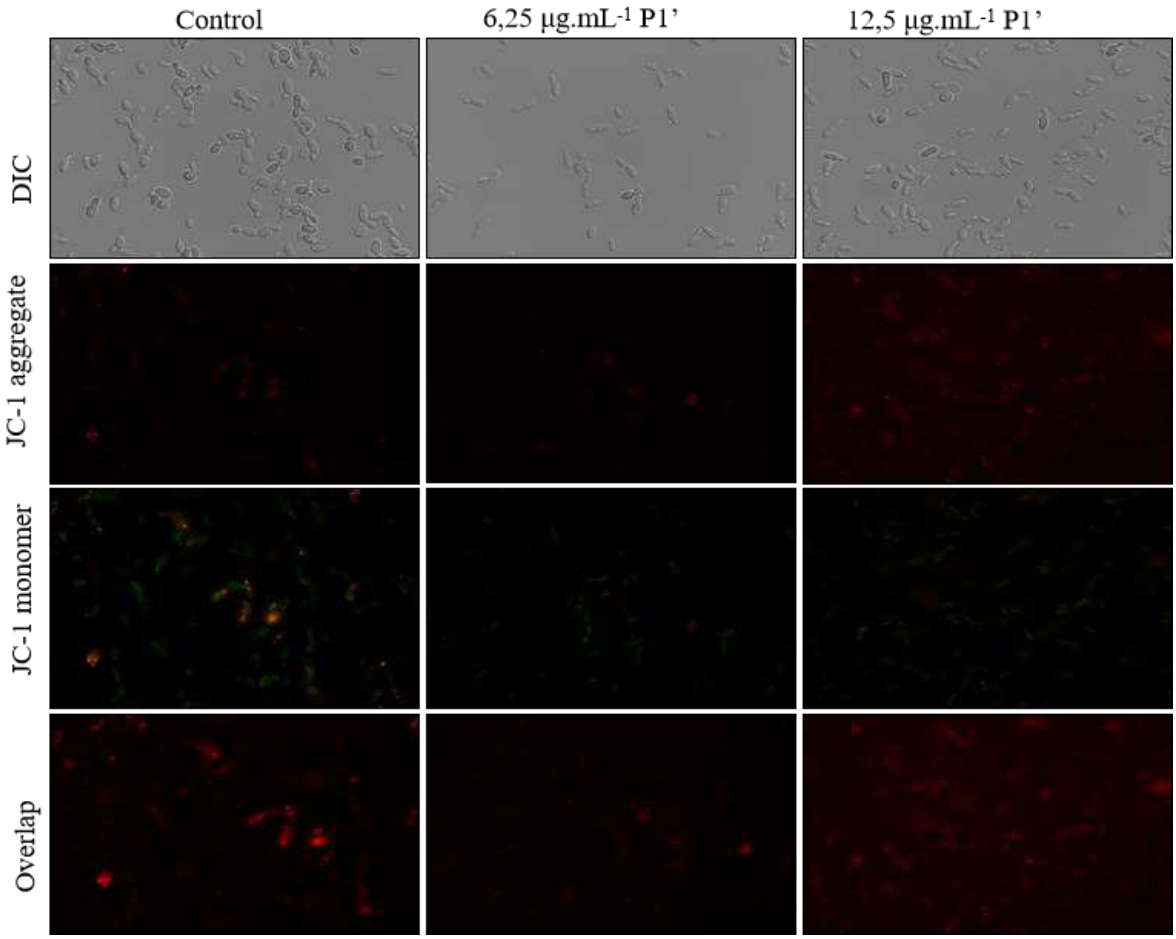

Fig. 8. Assessment of mitochondrial functionality in *C. tropicalis* after treatment with D-CDF-GK. Representative DIC and fluorescence microscopy images of yeast-phase *C. tropicalis* cells treated with 6,25 µg.mL-1 and 12,5 µg.mL-1 D-CDF-GK for 15 h and stained with JC-1. Untreated cells stained with JC-1 were used as the control. D-CDF-GK-treated cells showed reduced red fluorescence and a predominance of green fluorescence, indicating decreased mitochondrial membrane potential compared with untreated cells. Scale bars = 10 µm.

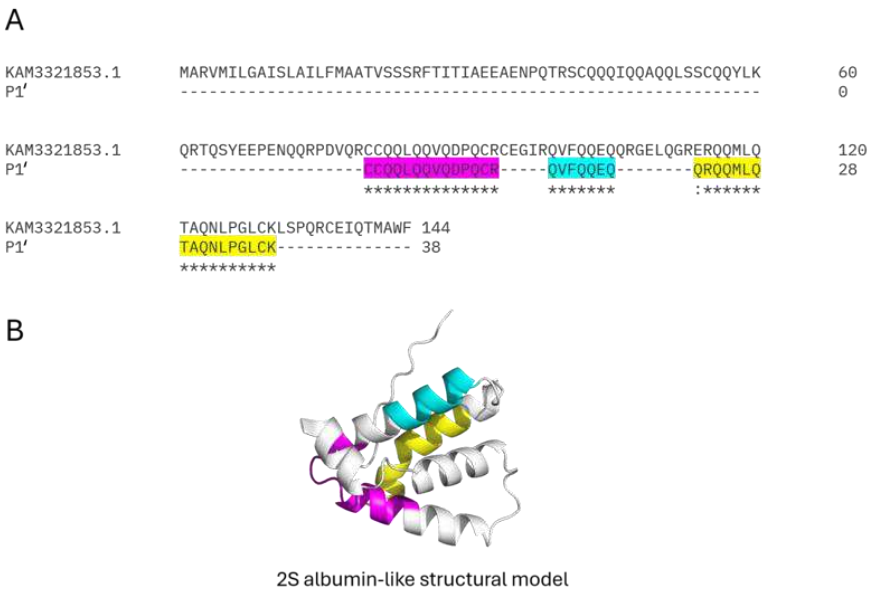

Fig. 9. Mapping of mass spectrometry-identified peptides onto the modeled 2S albumin-like protein. The three peptides identified in fraction P1' were aligned with the *Capsicum chacoense* hypothetical protein (KAM3321853.1) and are highlighted in magenta, cyan, and yellow. The corresponding regions were mapped onto the three- dimensional 2S albumin-like structural model using the same color scheme.

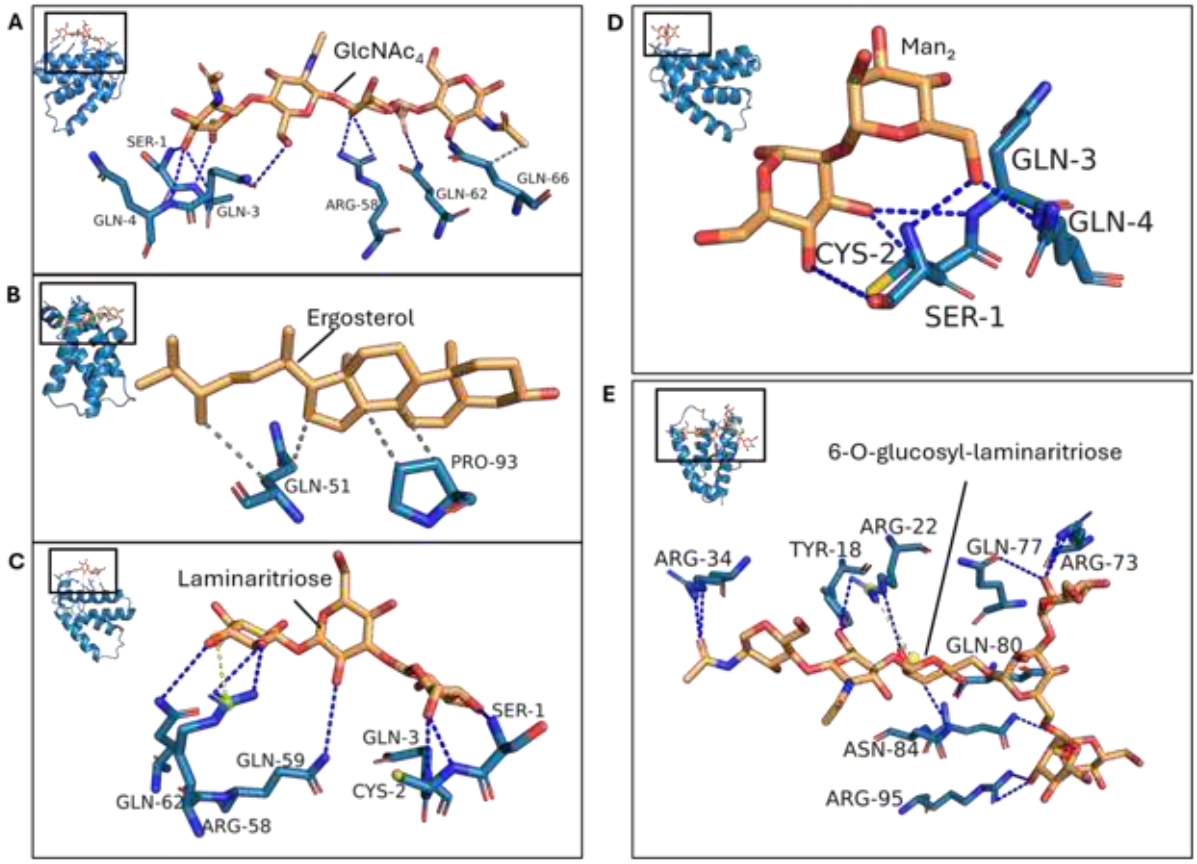

Fig. 10. Predicted molecular interactions between the 2S albumin-like model and selected fungal cell wall and membrane ligands. Representative docking poses and interacting residues identified by PLIP are shown for the complexes formed with (A) $GlcNAc_4$, (B) ergosterol, (C) laminaritriose, (D) Man_2 (α-1,2-mannobiose), and (E) 6-O-glucosyl-laminaritriose. The protein is shown in blue and ligands in orange. Dashed lines indicate the non-covalent interactions identified for each complex. Detailed interacting residues, interaction types, and distances are provided in Supplementary Table S1.

Table 1. Predicted binding affinities and molecular interactions of the 2S albumin-like protein with selected fungal cell wall and membrane ligands. Predicted affinity energies were obtained using DockThor, and molecular interactions were identified using PLIP. Interaction numbers correspond to the total number of contacts detected for each interaction type. Details regarding residues and interaction distances are presented in Supplementary Table S1.

Ligand name	Predicted affinity energy (kcal mol^{-1})	Hydrophobic interactions	Hydrogen bonds	Salt bridges
GlcNAc4	-8.736	1	9	0
Ergosterol	-9.006	4	0	0
Man2	-7.114	0	5	0
Laminaritriose	-8.064	0	7	1
6-O-glucosyl-laminaritriose	-9.195	0	15	1

Table S1. Predicted molecular interactions between the 2S albumin-like protein and selected fungal cell wall and membrane ligands. Residues listed correspond to amino acid residues of the modeled 2S albumin-like protein.

Ligand	Interaction type	Protein residue no.	Protein residue	Distance (Å) [a]
$(GlcNAc)_4$	Hydrophobic	66	GLN	3.92
$(GlcNAc)_4$	Hydrogen bonds	1	SER	1.76
$(GlcNAc)_4$	Hydrogen bonds	2	CYS	2.46
$(GlcNAc)_4$	Hydrogen bonds	3	GLN	2.60
$(GlcNAc)_4$	Hydrogen bonds	3	GLN	2.63
$(GlcNAc)_4$	Hydrogen bonds	4	GLN	2.98
$(GlcNAc)_4$	Hydrogen bonds	58	ARG	2.67
$(GlcNAc)_4$	Hydrogen bonds	58	ARG	2.17
$(GlcNAc)_4$	Hydrogen bonds	62	GLN	1.78
$(GlcNAc)_4$	Hydrogen bonds	66	GLN	2.16
Ergosterol	Hydrophobic	51	GLN	3.64
Ergosterol	Hydrophobic	51	GLN	3.98
Ergosterol	Hydrophobic	93	PRO	3.61
Ergosterol	Hydrophobic	93	PRO	3.73
Man_2	Hydrogen bonds	1	SER	1.92
Man_2	Hydrogen bonds	1	SER	3.43
Man_2	Hydrogen bonds	2	CYS	1.87
Man_2	Hydrogen bonds	3	GLN	3.10
Man_2	Hydrogen bonds	4	GLN	2.51
Laminaritriose	Hydrogen bonds	1	SER	2.04
Laminaritriose	Hydrogen bonds	2	CYS	2.18
Laminaritriose	Hydrogen bonds	3	GLN	2.23
Laminaritriose	Hydrogen bonds	58	ARG	2.79
Laminaritriose	Hydrogen bonds	58	ARG	2.05
Laminaritriose	Hydrogen bonds	59	GLN	3.43
Laminaritriose	Hydrogen bonds	62	GLN	2.90
Laminaritriose	Salt bridge	58	ARG	4.67
6-O-glucosyl-laminaritriose	Hydrogen bonds	18	TYR	2.75
6-O-glucosyl-laminaritriose	Hydrogen bonds	22	ARG	2.84
6-O-glucosyl-laminaritriose	Hydrogen bonds	22	ARG	3.05
6-O-glucosyl-laminaritriose	Hydrogen bonds	34	ARG	2.81
6-O-glucosyl-laminaritriose	Hydrogen bonds	34	ARG	2.41
6-O-glucosyl-laminaritriose	Hydrogen bonds	73	ARG	2.23
6-O-glucosyl-laminaritriose	Hydrogen bonds	73	ARG	2.44
6-O-glucosyl-laminaritriose	Hydrogen bonds	77	GLN	3.13
6-O-glucosyl-laminaritriose	Hydrogen bonds	80	GLN	3.14
6-O-glucosyl-laminaritriose	Hydrogen bonds	80	GLN	2.14
6-O-glucosyl-laminaritriose	Hydrogen bonds	83	GLN	2.83
6-O-glucosyl-laminaritriose	Hydrogen bonds	84	ASN	2.69
6-O-glucosyl-laminaritriose	Hydrogen bonds	95	ARG	2.26
6-O-glucosyl-laminaritriose	Hydrogen bonds	95	ARG	1.88

6-O-glucosyl-laminaritriose	Hydrogen bonds	95	ARG	2.74
6-O-glucosyl-laminaritriose	Salt bridge	22	ARG	5.10

1127